Heliyon 9 (2023) e18315

Contents lists available at ScienceDirect

Heliyon

journal homepage: www.cell.com/heliyon

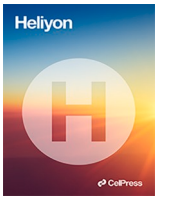

Serotonin increases population coding of behaviorally relevant stimuli by enhancing responses of ON but not OFF-type sensory neurons

Mariana M. Marquez, Maurice J. Chacron *

Department of Physiology, McGill University, Canada

ARTICLE INFO

Keywords:
Weakly electric fish
Population coding
Neuroethology
Serotonin
Neuromodulation

ABSTRACT

How neural populations encode sensory input to generate behavioral responses remains a central problem in systems neuroscience. Here we investigated how neuromodulation influences population coding of behaviorally relevant stimuli to give rise to behavior in the electrosensory system of the weakly electric fish *Apteronotus leptorhynchus*. We performed multi-unit recordings from ON and OFF sensory pyramidal cells in response to stimuli whose amplitude (i.e., envelope) varied in time, before and after electrical stimulation of the raphe nuclei. Overall, raphe stimulation increased population coding by ON- but not by OFF-type cells, despite both cell types showing similar sensitivities to the stimulus at the single neuron level. Surprisingly, only changes in population coding by ON-type cells were correlated with changes in behavioral responses. Taken together, our results show that neuromodulation differentially affects ON vs. OFF-type cells in order to enhance perception of behaviorally relevant sensory input.

1. Introduction

Understanding how behaviors are generated by the activities of neurons is a central question in neuroscience. Answering this question is complicated in part by the fact that the internal state of the brain is highly dynamic and neural responses are constantly adjusted via neuromodulators to generate appropriate behavior depending on context [1,2]. One such neuromodulator is serotonin, which modulates the activities of sensory neurons via fibers emanating from the raphe nuclei (see Refs. [3–6] for review). While previous studies have investigated the effects of serotonin on sensory processing using single unit recordings [7–13], it is now generally agreed that behavior is determined by combining the activities of large neural populations. This, together with technological advances permitting the simultaneous recording of the activities of large neural populations [14], has prompted multiple investigations of population coding and, particularly, how such coding is impacted by the fact that neural activities are not independent of one another (see Refs. [15–18] for review). However, how the activities of large neural populations are combined to give rise to behavior remains poorly understood in general [19]. Here we investigated how serotonin alters population coding of behaviorally relevant stimuli by sensory neurons and how changes in neural activity impact behavior.

Gymnotiform wave-type weakly electric fish offer an attractive model to study the effects of serotonin on population coding by sensory neurons and behavior. These fish detect amplitude modulations (AMs) of a self-generated electric field (i.e., the electric organ discharge or EOD) via electroreceptor afferents that relay this information to pyramidal cells within the electrosensory lateral line lobe

* Corresponding author.
E-mail address: maurice.chacron@mcgill.ca (M.J. Chacron).

https://doi.org/10.1016/j.heliyon.2023.e18315
Received 30 January 2023; Received in revised form 5 July 2023; Accepted 13 July 2023
Available online 14 July 2023

(ELL). Pyramidal cells project to higher order brain areas that generate behavior [20–22]. There are two main classes of ELL pyramidal cells: ON- and OFF-type cells. ON cells receive direct excitatory input from electroreceptor afferents, whereas OFF cells receive indirect inhibitory input via local interneurons. ON and OFF cells respond to increases in EOD amplitude with excitation and inhibition, respectively, when stimuli are delivered either locally within the center portion of their receptive fields or globally across their entire

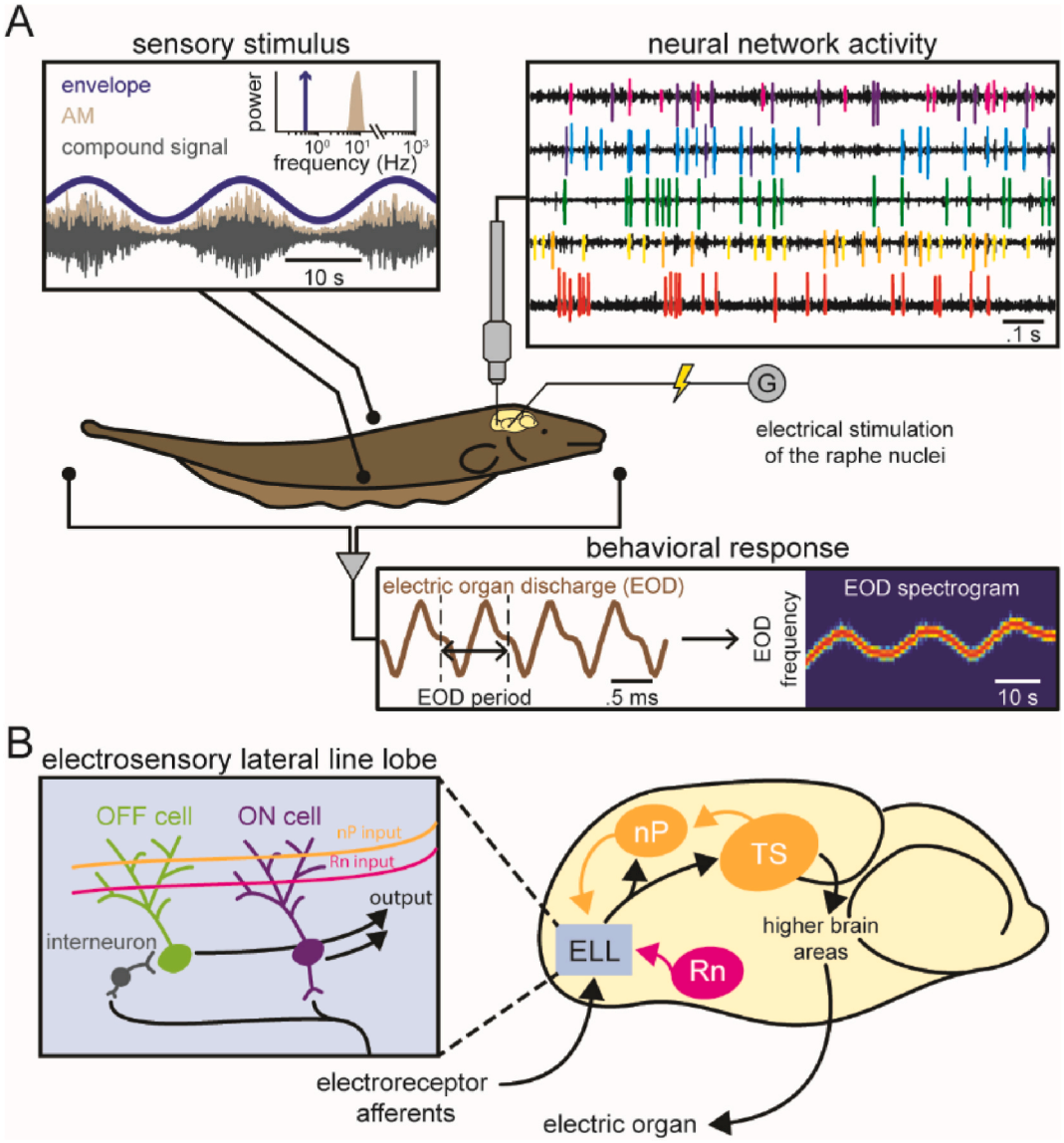

Fig. 1. Experimental set up and relevant circuitry. **A)** Schematic showing the experimental setup where multi-unit recordings were made from awake behaving fish using Neuropixel probes. Sorted action potentials of different neurons are highlighted in different colors for recordings on five example channels (top right). The stimulus consisted of amplitude modulations of the fish's electric organ discharge (EOD). Shown are the compound signal received by the animal (grey), the amplitude modulation of that signal (AM, light grey) and its envelope (blue), as well as their respective frequency contents (inset). We used a pair of electrodes perpendicular to the fish's rostro-caudal axis to deliver the stimuli and monitored the animal's behavioral responses through a separate pair of electrodes located near the snout and tail. Behavioral responses consisted of changes in the electric organ discharge (EOD) frequency (bottom). Shown are the fish's EOD (brown) on the left and the EOD spectrogram on the right showing EOD frequency modulation in response to the envelope stimulus (blue trace in upper left). Electrical stimulation of the Raphe nuclei was achieved through a stimulus generator (G) connected to stimulation electrodes placed within the brain. **B)** Simplified diagram showing relevant brain areas in the electrosensory system. EOD AMs are encoded by electroreceptor afferents that project directly to ON cells and indirectly via local inhibitory interneurons to OFF cells in the electrosensory lateral line lobe (ELL), the first stage of sensory processing in the central nervous system. The ELL, in turn, projects to the nucleus praeeminentialis (nP) which feeds back to ELL and the torus semicircularis (TS) which, besides also sending feedback to the ELL, sends information to higher brain areas that control the electric organ and give rise to behaviors. The ELL, among other brain areas, receives serotonergic input from the Raphe nuclei (Rn). (For interpretation of the references to color in this figure legend, the reader is referred to the Web version of this article.)

receptive fields [23–25]. Additionally, both ON and OFF cells display large heterogeneities in terms of dendritic morphology, presence and distribution of membrane conductances, and firing characteristics (see Ref. [26] for review), which contribute to differential responses to stimulation (see Refs. [27–29] for review). When two conspecific fish are in proximity to each other, interference between their EODs gives rise to a sinusoidal AM (i.e., a beat) whose amplitude (i.e., the envelope) varies as a function of the relative distance

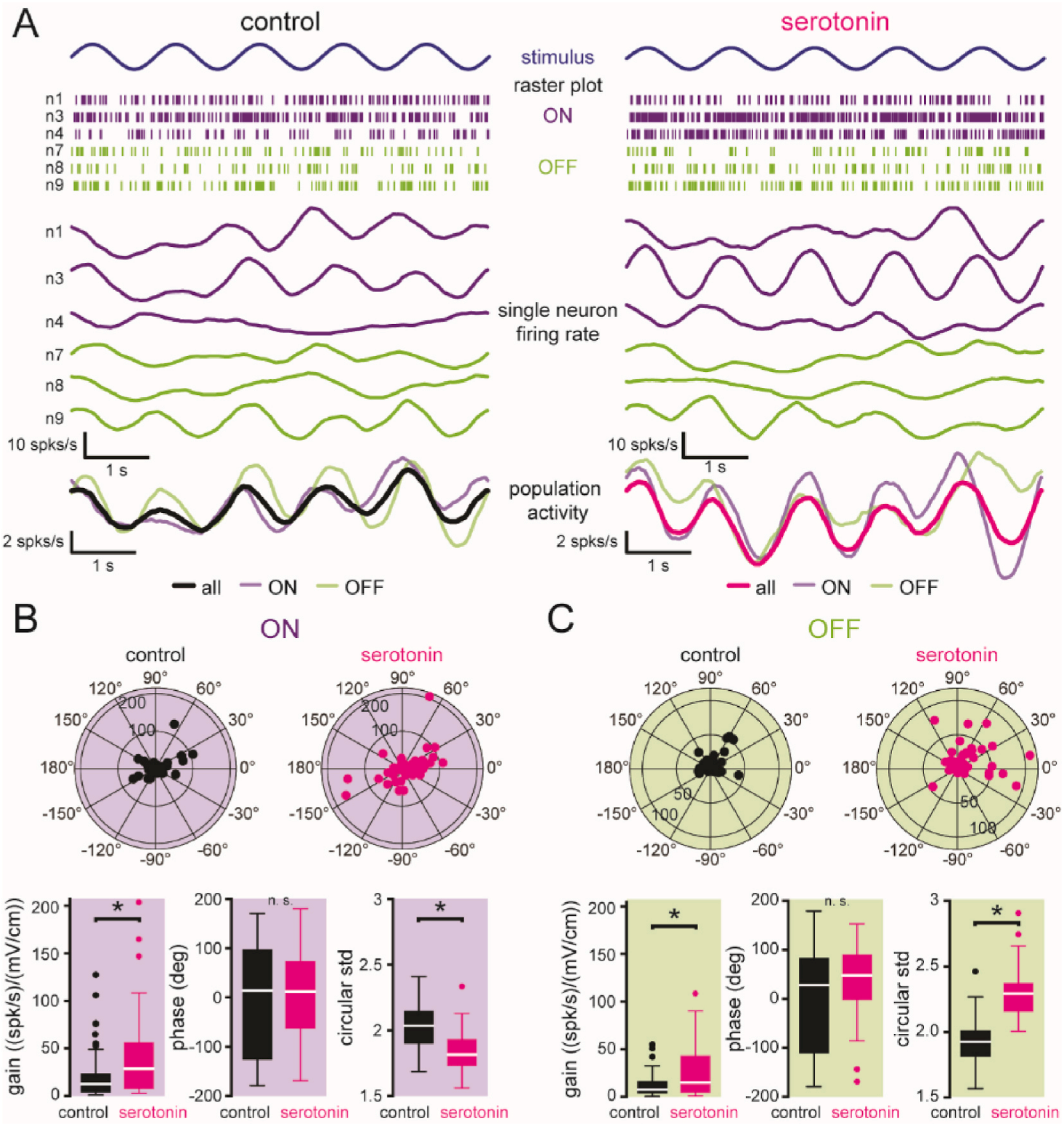

Fig. 2. Serotonin differentially modulates the responses of ON vs. OFF cell populations. A) Envelope stimulus (top, .75 Hz), raster plots (middle top) and time-dependent firing rates (middle bottom) showing responses of 5 example ON (purple) and 5 example OFF (green) cells, as well as population activities from ON (light purple), OFF (light green), and all (black) cells (bottom) under control (left) and after raphe stimulation (right, magenta). Note that modulations of the time-dependent firing rate of individual neurons, as well as the summed network activity (magenta), are more evident after raphe stimulation. **B)** Top, polar plots showing neural sensitivity (radial axis) and preferred phase (angular axis) to all envelope frequencies (n = 18 neurons for six different envelope frequencies) during control (left, black dots) and after raphe stimulation (right, magenta dots) for the ON cell population. Bottom, raphe stimulation significantly increased the sensitivity or gain ($p = 2.4 \times 10^{-9}$, Wilcoxon's signed-rank) of the ON cell population. Preferred phase values were not statistically different from control ($p = 0.78$, Wilcoxon's signed-rank). Here, positive/negative values imply that the neural response leads/lags the stimulus. Circular standard deviation (circular std) significantly decreased ($p = 7.4 \times 10^{-7}$, Student's t-test, n = 50, bootstrapped) after raphe stimulation. **C)** Same as B) but for the OFF cell population. Raphe stimulation significantly increased the sensitivity to envelopes ($p = 7.4 \times 10^{-6}$, Wilcoxon's signed-rank), while it did not significantly affect the preferred phase ($p = 0.14$, Wilcoxon's signed-rank). Circular standard deviation significantly increased after raphe stimulation ($p = 1.9 \times 10^{-9}$, Wilcoxon's signed-rank, n = 50, bootstrapped). These results indicate that neural responses of ON cells became more homogeneous and neural responses of OFF cells became more heterogeneous after stimulation of the raphe nuclei. (For interpretation of the references to color in this figure legend, the reader is referred to the Web version of this article.)

and orientation between two fish (see Refs. [30,31] for review). Information as to the time-varying envelope is retained in the brain, as these fish display changes in their EOD frequency that track the detailed timecourse of the envelope stimulus [32]. Previous studies have investigated how electrosensory neurons, including ELL pyramidal cells, respond to envelope stimuli, but have relied on single-unit recordings [33–38]. ELL pyramidal cells also receive serotonergic innervation from the raphe nuclei [39,40]. Previous studies have shown that activation of serotonergic pathways increases the excitability of single ELL pyramidal cells [40–42], which makes them more responsive to sensory input including envelope stimulation [43,44] (see Ref. [45] for review). While recent studies have started to investigate how electrosensory neural populations encode electrocommunication stimuli [46,47], how these populations encode envelope stimuli, and the effects of neuromodulators on such coding, has not been investigated to date.

To answer this question, we used high-density arrays (i.e., Neuropixels probes) to record the simultaneous activities of ELL pyramidal cell populations in response to envelope stimuli before and after electrical stimulation of the raphe nuclei in awake behaving fish. We found that serotonin affected the heterogeneity of responses and the trial-to-trial variability of ON and OFF pyramidal cells in differential fashion, such that information as to the timecourse of the envelope stimulus was primarily, if not exclusively, carried by the ON subpopulation. Further analysis revealed that changes in behavior due to raphe stimulation were best predicted by only considering the activities of ON cells. Taken together, our results show for the first time that raphe stimulation leads to asymmetric coding by two neural subpopulations to give rise to behavior. Based on important similarities between the electrosensory and other systems [48], and the fact that the serotonergic system is conserved across vertebrate species [49], our results will likely be applicable elsewhere.

2. Results

We investigated the effects of electrical stimulation of serotonergic fibers on the sensory coding of envelope stimuli by population of pyramidal neurons in the hindbrain ELL. The experimental preparation we used is schematized in Fig. 1. Specifically, we inserted a high-density electrode array in the brain to record the activities of ELL pyramidal cell populations while simultaneously using external electrodes to record the animal's behavioral responses, consisting of changes in the EOD frequency to sensory stimulation (Fig. 1A bottom). Our stimuli consisted of noisy amplitude modulations of the fish's own EOD whose amplitude (i.e., the envelope) varied sinusoidally at different frequencies spanning the physiologically relevant range. The top left panel of Fig. 1A shows the envelope waveform (blue), the noisy carrier (light grey) and the compound signal that is delivered in the water (dark grey) as well as their respective frequency contents (inset). We are considering both first- (i.e., amplitude modulation) and second-order (i.e., envelope) features of the stimulus and note that these correspond to the second- and third-order features of the full signal received by the animal, respectively. Thus, the first-order feature corresponds to the mean and the second-order feature corresponds to the variance of the stimulus.

Ascending electrosensory pathways are schematized in Fig. 1B. Electroreceptor afferents project to ELL pyramidal cells which, as previously mentioned, can be classified as ON or OFF based on their responses to changes in EOD amplitude (Supplementary Fig. 1). ON and OFF pyramidal cells in turn project directly to the nucleus praeeminentialis (nP) and midbrain torus semicircularis (TS). TS projects to higher brain areas that mediate behavior, while projections from both TS and nP give rise to feedback input to the ELL. ELL pyramidal cells also receive descending input from the raphe nuclei (Rn) [39]. It is important to note that ON and OFF cells respond to the AM stimuli in opposite fashion, with ON cells responding with increased firing activity to increases in EOD amplitude and OFF cells responding with increased firing activity to decreases in EOD amplitude [24,50]. However, this is not the case when one considers the envelope, which varies more slowly than the AM stimulus. As such, it is possible to have ON and OFF cells both respond to increases in the envelope and at the same time responding to increases and decreases in the AM stimulus, respectively [50].

2.1. Serotonin differentially modulates ON and OFF subpopulation responses to envelope stimuli

We first investigated how raphe stimulation altered responses of ELL pyramidal cells to envelope stimuli. Overall, these responses were highly heterogeneous under control conditions (i.e., before raphe stimulation), with both ON and OFF cells firing preferentially at different phases of the envelope stimulus (e.g., compare the firing activities of neurons 3,4, and 7 in Fig. 2A left). Overall, raphe stimulation increased pyramidal cell excitability in the absence of stimulation, as quantified by increased firing rate and burst firing (Supplementary Fig. 2), consistent with previous results [41]. Raphe stimulation increased ELL pyramidal cell sensitivity as evidenced by an overall greater modulation in firing rate (Fig. 2A right).

As the firing rates of neurons varied sinusoidally with the envelope before and after raphe stimulation, we used linear systems identification techniques to compute response sensitivity and preferred phase (Fig. 2B and C). We found that raphe stimulation significantly increased neural sensitivity for both ON and OFF cells but did not affect neurons' preferred phase (Fig. 2B and C bottom). Interestingly however, polar plots of gain and phase revealed more heterogeneous responses after raphe stimulation for OFF but not for ON cells (Fig. 2B and C top). Indeed, while in control conditions OFF cells fired at a similar phase, serotonin rendered their responses more out of phase of each other (e.g., compare neurons 7 and 8 in Fig. 2A). On the other hand, more ON cells fired at the same preferred phase after raphe stimulation (e.g., compare neurons 3 and 4 in Fig. 2A). Changes in response heterogeneity were quantified using the circular STD (see Methods), with higher values indicating more heterogeneity. Overall, the circular STD was significantly decreased after raphe stimulation for ON cells (Fig. 2B, bottom) but was instead significantly increased for OFF cells (Fig. 2C, bottom) (ON: $p = 0.03$, Wilcoxon's signed-rank, OFF: $p = 5.1 \times 10^{-9}$, Wilcoxon's signed-rank). When comparing ON and OFF cells (Supplementary Fig. 3), we found that these displayed overall similar response properties to the envelope before raphe stimulation as quantified by gain ($p = 0.09$, Wilcoxon rank sum test) and phase ($p = 0.22$, Wilcoxon rank sum test), which is consistent with previous results [33,51]. Interestingly, circular STD for ON cells was slightly lower than for OFF cells ($p = 0.012$, Student's t-test). After raphe stimulation, both

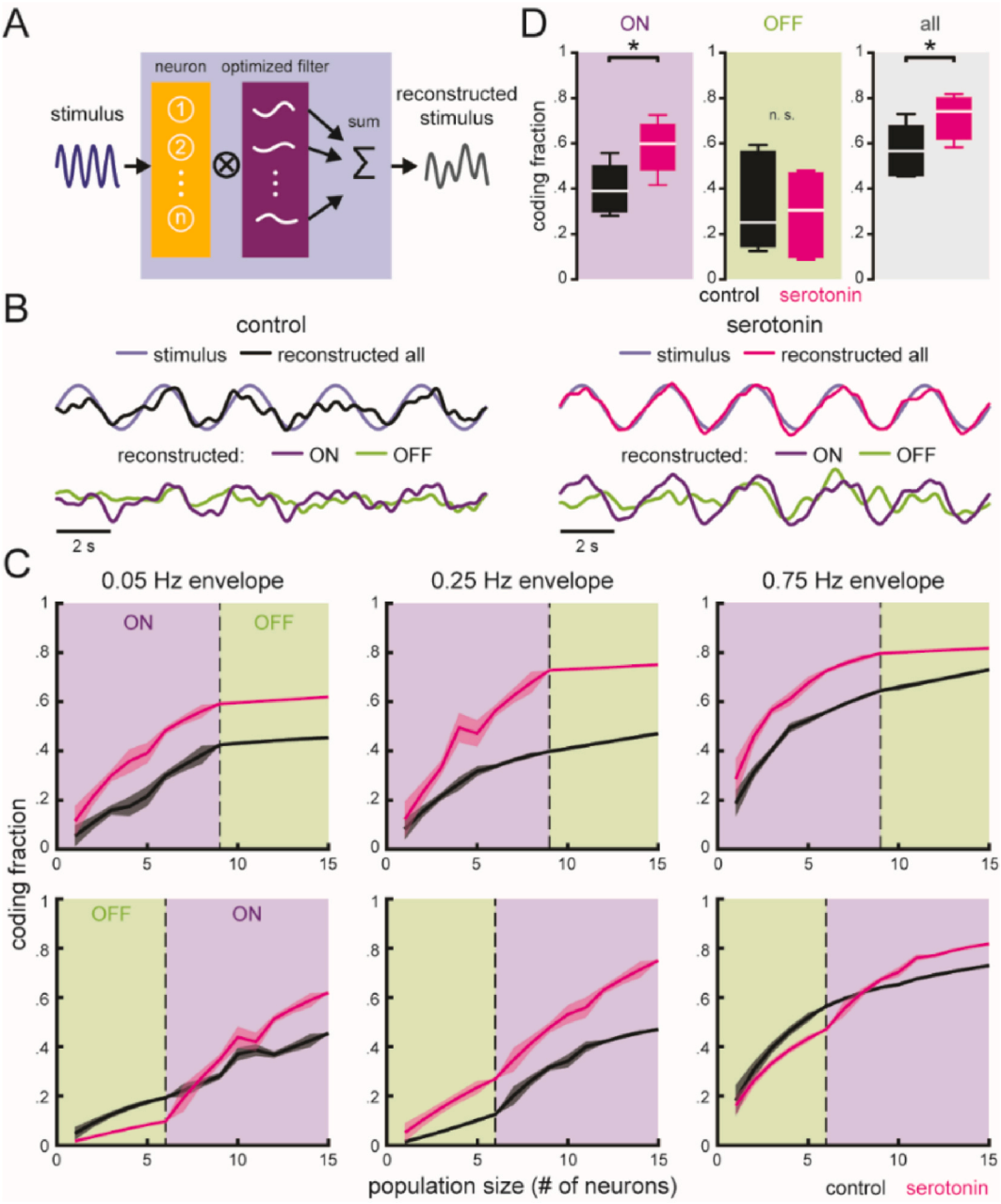

Fig. 3. Information about the envelope stimulus' timecourse is primarily encoded by ON cells. A) Schematic of the linear decoder considered here. The activity of each neuron is convolved with an optimized filter, the convolved neural responses are then added together to obtain the reconstructed stimulus. The filters selected are those that minimize the mean square error between the original stimulus and the reconstructed one. **B)** Example traces of the stimulus estimated from a population of 12 neurons during control (black, left) and after raphe stimulation (magenta, right) overlapped with the actual stimulus (fainted blue, 0.25 Hz envelope). Shown below is the same example but computed only from the contributions of ON cells (6 neurons, purple trace) and OFF cells (6 neurons, green trace). Note that the quality of the reconstruction increases after raphe stimulation mostly due to the enhanced contributions from ON cells. **C)** Coding fraction as a function of population size for different envelope frequencies during control (black traces) and after raphe stimulation (magenta traces). Top, the reconstruction is calculated by pooling ON cells first (purple background) and then OFF cells (green background). Bottom, the reconstruction is calculated by pooling OFF cells first instead. **D)** Coding fraction at the maximum population size for all stimulus conditions. The coding fraction is significantly larger after raphe stimulation when all cells are considered for the reconstruction, as well as when only ON cells are included, but not when only OFF cells are included (ON: $p = 2.8 \times 10^{-4}$, Student's t-test; OFF: $p = 0.06$, Student's t-test; all cells: $p = 0.03$, Wilcoxon's signed-rank). (For interpretation of the references to color in this figure legend, the reader is referred to the Web version of this article.)

ON and OFF cells displayed similar gain ($p = 0.08$, Wilcoxon rank sum test) and phase ($p = 0.048$, Wilcoxon rank sum test) values, which is expected because raphe stimulation increases gain similarly for both ON and OFF cells and does not affect phase values much. OFF cells displayed higher circular STD values than ON cells ($p = 1.06 \times 10^{-17}$, Student's t-test) after raphe stimulation, which is expected as raphe stimulation has opposite effects on circular STD for ON and OFF cells. These results demonstrate that raphe stimulation has differential effects on the activities of ON and OFF pyramidal cells by decreasing and increasing response heterogeneity in the former and latter cases, respectively.

2.2. *Raphe stimulation promotes asymmetric coding of envelope stimuli by ON and OFF cell subpopulations*

How does raphe stimulation alter population coding of envelope stimuli by ELL pyramidal cells? To answer this question, we considered the performance of an optimized linear decoder towards reconstructing the detailed timecourse of the stimulus (Fig. 3A). Briefly, each spike train is convolved with a separate filter and a summation is then performed over neurons to obtain the reconstructed stimulus. The filters are chosen such as to minimize the mean-square error between the original and reconstructed stimuli and the use of separate filters can better account for response heterogeneities observed in the data above (Fig. 2A and B). The quality of the reconstruction was quantified by the coding fraction, which ranges between 0 and 1 and represents the fraction of the stimulus that is correctly reconstructed (see Methods). The use of the stimulus reconstruction appears justified here because the animal's behavioral response follows the detailed timecourse of the envelope stimulus, indicating that information about such timecourse must be retained

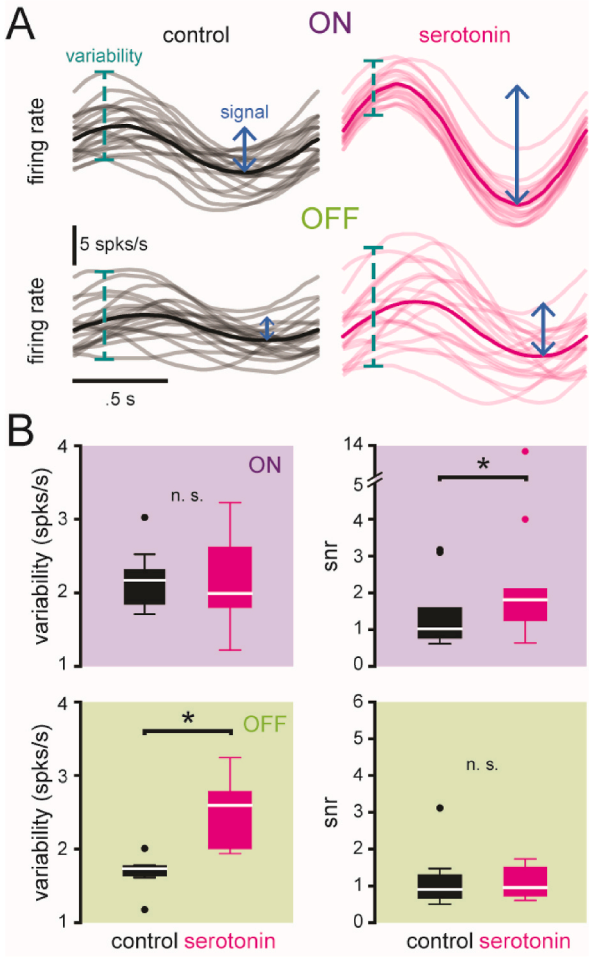

Fig. 4. Serotonin differentially affects trial-to-trial variability of ON and OFF cells. A) Top, time dependent firing rate of a representative ON cell during 20 envelope cycles superimposed with the mean firing rate across all trials (solid line) during control condition (black, left) and after raphe stimulation (magenta, right). The blue arrows show the amplitude of the mean firing rate (signal). The turquoise dotted lines show the variability of the response (absolute difference between each trial response and the mean response). Bottom, same but for a representative OFF cell. **B)** Top, box plots showing the variability and the signal to noise ratio (snr i.e., signal to variability ratio, see Methods) computed from all the ON cells recorded during control (black) and after raphe stimulation (magenta) (variability: $p = 0.95$, Student's t-test; snr: $p = 0.01$, Wilcoxon's signed-rank). Bottom, same but for OFF cells (variability: $p = 0.02$, Student's t-test; snr: $p = 0.8$, Wilcoxon's signed-rank). (For interpretation of the references to color in this figure legend, the reader is referred to the Web version of this article.)

in the brain [32].

Overall, under control conditions, we found that while the combined activities of ELL pyramidal cell populations carried information as to the stimulus' detailed timecourse (Fig. 3B left panel, compare light blue and black traces), ON and OFF cells contributed differentially to the quality of the reconstruction despite showing similar sensitivities and phase relationships to envelopes (Fig. 2C). Indeed, only considering the activities of ON cells led to much better reconstruction than only considering the activities of OFF cells (Fig. 3B left panel, compare purple and green traces to light blue trace). This asymmetry was reflected in plots of the coding fraction as a function of population size for different envelope frequencies (Fig. 3C and Supplementary Fig. 4, black traces). When first considering ON cells only, the coding fraction rapidly increased with population size but then saturated when OFF cells were added (Fig. 3C and Supplementary Fig. 4, black traces in top panels). Instead, when first considering OFF cells only, the coding fraction only increased marginally but then more strongly increased only when ON cells were added (Fig. 3C and Supplementary Fig. 4, black traces in bottom

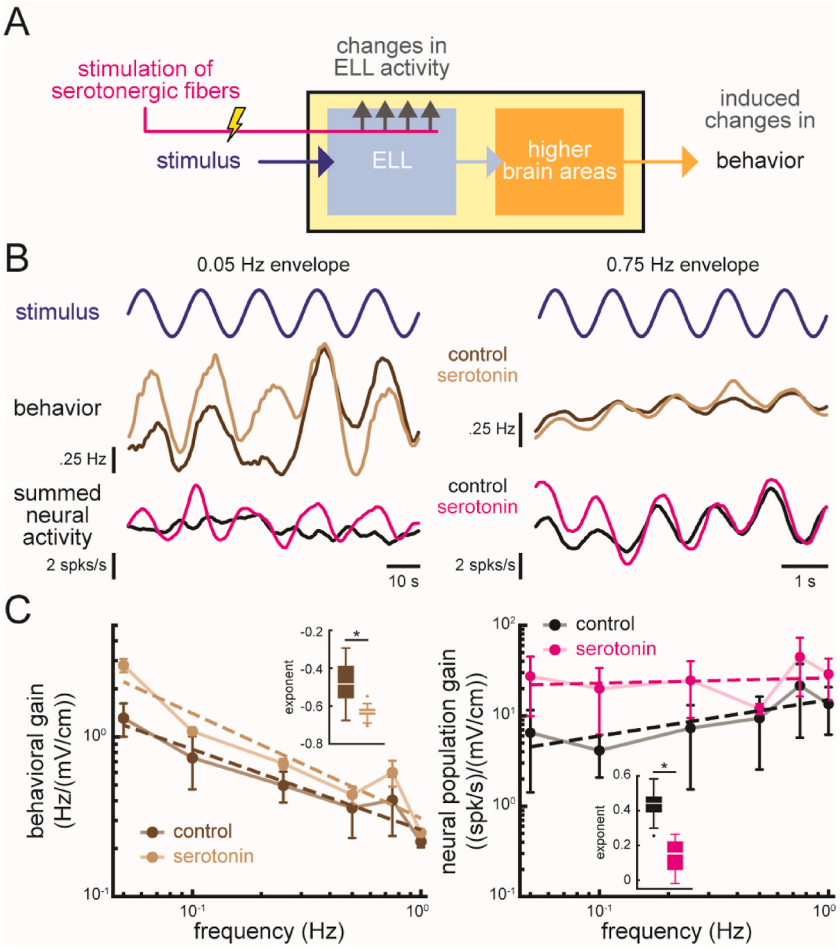

Fig. 5. A simple sum of the activities of all neurons cannot predict changes in behavioral responses after raphe stimulation. A) Information about the envelope stimulus is processed across multiple brain areas to give rise to behavior, but electrical stimulation of serotonergic fibers that innervate the ELL is enough to induce changes in ELL pyramidal cell responses and behavioral responses to envelopes, as is exogenous application of serotonin [43]. How changes in neuronal responses generate changes in behavior is not understood yet. **B)** Left, representative behavioral response (middle) and summed neural activity (bottom) to a 0.05 Hz sinusoidal envelope (top, blue) for control (dark brown and black respectively) and after raphe stimulation (light brown and magenta respectively). Right, same but in response to a higher frequency envelope (0.75 Hz). Note the difference between behavioral responses and the summed neural activity: while the behavioral response is larger for the low frequency envelope and diminishes for the high envelope frequency, the summed neural activity is modulated in response to the high envelope frequency, but not the low envelope frequency. Raphe stimulation primarily enhances behavioral response to the low envelope frequency, but it enhances the modulation of the summed neural activity to the two envelope stimuli. For better visualization, the behavioral responses were low pass filtered with a 1 s and 225 ms width box car respectively. **C)** Left, normalized behavioral sensitivity as a function of envelope frequency for control (dark brown) and after raphe stimulation (light brown). The dotted lines show the best power law fits to the data. Inset, averaged best-fit power law exponent significantly decreases after raphe stimulation ($p = 1.49 \times 10^{-14}$, Wilcoxon's signed-rank, bootstrapped from two experiments). Right, same but for the summed neural activity ($p = 5.61 \times 10^{-9}$, Wilcoxon's signed-rank, bootstrapped from two experiments). While both behavioral and neural power law exponents become more negative, the behavioral tuning curve is low-pass whereas the summed neural tuning curve is, at best, constant as a function of envelope frequency. (For interpretation of the references to color in this figure legend, the reader is referred to the Web version of this article.)

panels).

Interestingly, we found that raphe stimulation further exacerbated the differential contributions of ON and OFF cell subpopulations towards reconstructing the detailed timecourse of envelope stimuli (Fig. 3B right panel, compare purple and green traces to those on the left panel). Indeed, coding fraction was increased only when ON cells were included (Fig. 3C and Supplementary Fig. 4, magenta traces). Taken together, these results show that raphe stimulation differentially affects information transmission by ON and OFF cells. Specifically, the overall information content carried by the ELL pyramidal cell population is increased after raphe stimulation because the information content of ON, but not OFF cell subpopulations is increased. This effect was observed across envelope frequencies (Fig. 3C and 3D, and Supplementary Fig. 4).

2.3. Raphe stimulation differentially alters trial-to-trial variability in ON and OFF ELL pyramidal cell populations

How can raphe stimulation increase the information content of ON but not OFF ELL pyramidal cell populations, despite having similar effects on their sensitivities at the single neuron level? To answer this question, it is important to consider that information is not solely determined by neural sensitivity, but also by variability [52]. As such, we investigated the effects of raphe stimulation on the trial-to-trial variability of responses to envelopes for ON and OFF cells. Fig. 4A shows the responses of representative ON and OFF cells. During control condition, we observed that the modulated responses have a similar degree of trial-to-trial variability for both cells (compare the dotted turquoise lines on the left). However, after raphe stimulation, the ON cell's responses to repeated stimulation were more similar across trials, indicating decreased trial-to-trial variability, whereas the OFF cell's responses to repeated stimulation were more variable, indicating increased trial-to-trial variability. When looking at the entire dataset, raphe stimulation significantly increased trial-to-trial variability for OFF but not ON cells (Fig. 4B left, top and bottom respectively). We next computed the signal-to-noise ratio (snr, see Methods) and found increases after raphe stimulation for ON, but not OFF cells (Fig. 4B right, top and bottom respectively). This is because the increased sensitivity after raphe stimulation (Fig. 2B and C) is offset for OFF but not ON cells. When comparing ON and OFF cells before raphe stimulation (Supplementary Fig. 3), there were no differences in variability ($p = 0.40$, Wilcoxon rank sum) and snr ($p = 0.60$, paired Student's t-test). After raphe stimulation, OFF cells displayed higher variability than ON cells ($p = 0.04$, Wilcoxon rank sum test), which is expected given that raphe stimulation increases variability for OFF but not ON cells. There were no snr differences between ON and OFF cells after raphe stimulation ($p = 0.15$, Wilcoxon rank sum test).

2.4. Raphe stimulation increases correlations between ELL pyramidal cell activities

In general, information carried by neural populations can be strongly influenced by signal (i.e., the similarity between neural responses that are attributable to a common stimulus) and noise (i.e., the similarity between the trial-to-trial variabilities of neural responses) correlations [17]. As such, we quantified both quantities before and after raphe stimulation (see Methods). Overall, we found that raphe stimulation increased the magnitude of both signal and noise correlations between ELL pyramidal cell pairs (Supplementary Fig. 5). However, the contribution of noise correlations to the total information encoded by the ELL neural population was negligible since removing them from the population activities did not significantly change the coding fraction (Supplementary Fig. 6). Thus, the differences in coding fraction observed between ON and OFF cells are due to changes in single neuron attributes (e.g., sensitivity and snr), rather than changes in correlations.

2.5. A linear decoder that sums up the activities of all neurons cannot predict changes in behavioral responses to envelopes induced by serotonin

How do changes in the activities of ELL pyramidal neurons induced by raphe stimulation determine changes in the animal's behavioral responses (Fig. 5A)? To answer this question, it is important to note that behavioral responses are non-trivially related to neural responses. Indeed, under control conditions, behavioral sensitivity (i.e., gain) to envelope stimuli decreased as a function of envelope frequency, indicating low-pass tuning (Fig. 5B middle panels, dark brown trace and Fig. 5C left panel, dark brown trace), whereas the sensitivity of the summed neural activity (i.e., the neural population) instead increased with envelope frequency, indicating high-pass tuning (Fig. 5B bottom panels, black trace and Fig. 5C, right panel, black trace). After raphe stimulation, both behavioral and neural population sensitivity increased (Fig. 5B, compare magenta and light brown traces to black and dark brown traces, respectively). However, behavioral gain increased more for low than for high frequencies, leading to a steeper decrease with increasing frequency (Fig. 5C left panel, light brown). In contrast, neural population sensitivity became largely independent of frequency (Fig. 5C right panel, magenta). Behavioral and neural tuning curves were fitted with a power law and lower power law exponents were obtained in both cases (Fig. 5C insets). We found that the change in exponent obtained for behavior after raphe stimulation did not numerically correspond to the change in exponent observed for the neural population activity (Fig. 5C insets). Thus, these results show that behavioral responses are most likely not determined by simply adding the spiking activities of ELL pyramidal cells in the manner described above.

2.6. An optimized linear decoder that includes the activities of ON pyramidal cells best predict changes in behavioral responses to envelopes induced by serotonin

We used an optimized linear decoder as described above to quantify how the animal's behavioral response can be reconstructed based on the activities of ELL pyramidal cells (Fig. 6A). Overall, performance improved after raphe stimulation, but this improvement

was primarily observed for ON rather than OFF subpopulations (Fig. 6B). Moreover, in relative terms, improvement was greater for low envelope frequencies (compare Fig. 6B left and right panels). Overall, quantification of performance using the coding fraction revealed an overall increase for ON but an overall decrease for OFF cells, such that the coding fraction obtained from all cells either increased or decreased with envelope frequency (Fig. 6C–E black traces). Importantly, after raphe stimulation, the quality of the reconstruction is enhanced only for low envelope frequencies when considering the activities of all cells (Fig. 6C), indicating that this is due to the increased coding fraction for ON cells, as opposed to the decreased coding fraction for OFF cells.

To compare changes in neural population activity to changes in behavior induced by raphe stimulation, we computed the relative

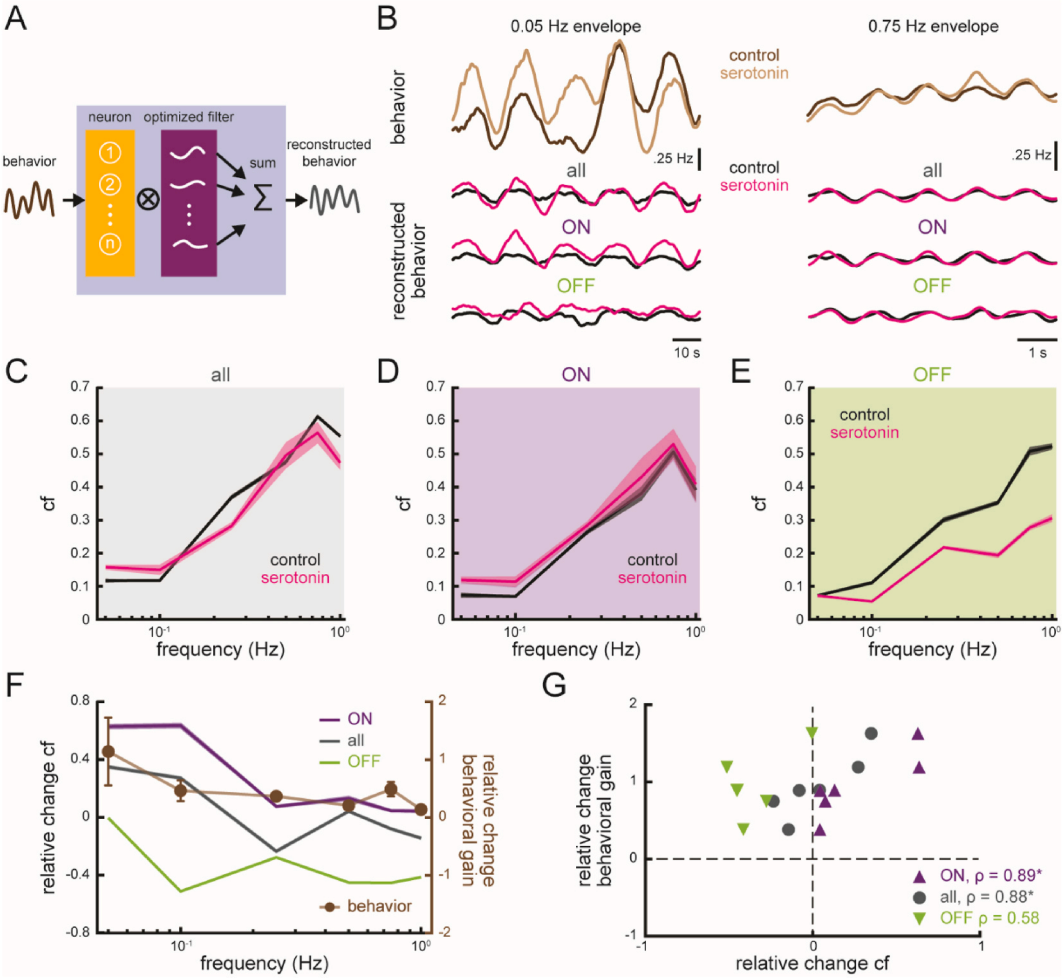

Fig. 6. ON cells best predict changes in behavior responses after raphe stimulation. A) Schematic of the linear decoder used to predict behavioral responses. Similarly to what was done to reconstruct the envelope stimuli, the neural activities are convolved with an individual optimized filter and then added together to obtain the best reconstruction of behavior. The filters selected are those that minimize the mean square error between the original behavioral response and the reconstructed one. **B)** Left top, representative behavioral response to a 0.05 Hz envelope (blue) during control (light brown) and after raphe stimulation (dark brown). Shown below is the behavior reconstructed from the activities of all cells, ON cells and OFF cells only during control (black) and after raphe stimulation (magenta). Right top, same as on the left side but for a 0.75 Hz envelope. Note that the reconstruction of behavior is improved after raphe stimulation and that this improvement is more evident when the estimation is done from the activities of ON cells only. **C)** Coding fraction as a function of envelope frequency when the behavior is reconstructed from the activities of all cells (n = 8) during control (black) and after raphe stimulation (magenta). **D)** Same as C), but when the reconstruction is computed from the activities of ON cells only (n = 4). **E)** Same as C), but when the reconstruction is computed from the activities of OFF cells only (n = 4). **F)** Relative change in coding fraction as a function of envelope frequency when the reconstruction of behavior is computed from the activities of all cells (grey), ON cells (purple) and OFF cells (green) only. Superimposed is the relative change in behavioral gain as a function of envelope frequency (brown). Behavioral error bars are computed through bootstrapping technique (see Methods). **G)** Relative change in behavioral gain plotted against the relative change in coding fraction associated with the reconstruction computed from all cells (grey circles), ON cells (purple triangles) and OFF cells (green inverted triangles) only. We found a significant correlation between the relative change in behavioral gain and coding fraction associated with all cells ($p = 0.02$, Pearson correlation) and ON cells ($p = 0.03$, Spearman correlation), but not OFF cells ($p = 0.23$, Pearson correlation), as indicated by *. (For interpretation of the references to color in this figure legend, the reader is referred to the Web version of this article.)

changes in behavioral sensitivity and coding fraction as a function of envelope frequency (Fig. 6F). Overall, we found that the dependency of the relative change in coding fraction with envelope frequency was most similar to the relative change in behavioral sensitivity when only ON cells were considered (Fig. 6F, compare purple and brown traces), followed by all cells (Fig. 6F, compare grey and brown traces), followed by OFF cells (Fig. 6F, compare green and brown traces). Indeed, the relative change in coding fraction obtained from OFF cells was negative and thus opposite to the increased relative change in behavioral sensitivity. Overall, we found a significant positive correlation between the relative changes in behavioral sensitivity and coding fraction by all cells and ON cells, but not OFF cells (Fig. 6G). This indicates changes in the activities of ON type cells best predict changes in behavior, suggesting that downstream decoders are already tuned to asymmetric coding of envelope stimuli by ON and OFF cell subpopulations.

3. Discussion

3.1. Summary of results

We investigated how serotonin alters population coding of envelope stimuli by ELL pyramidal cells and how information about the stimulus' detailed timecourse is decoded in order to generate behavior. At the single neuron level, raphe stimulation increased neural excitability and sensitivity to envelopes for both ON and OFF cells but had opposite effects by making the responses of ON cells more homogeneous and those of OFF cells more heterogeneous. At the population level, we found that information about the envelope stimulus' detailed timecourse was carried mostly by ON cells. After raphe stimulation, ON cells carried even more information about the stimulus' detailed timecourse whereas the information carried by OFF cells was not increased. Further analysis revealed that this was because raphe stimulation increased the response trial-to-trial variability for OFF but not ON cells, thereby offsetting the beneficial effects of increased sensitivity in the former but not the latter case. Changes in information content were due to changes in single neuron properties, as opposed to changes in noise correlations. Finally, we investigated how the activities of ELL pyramidal cell populations determined behavioral responses at the organismal level. Overall, our results showed that changes in the activities of ON cells were the best predictor of behavioral responses. Taken together, our results show that serotonin further exacerbates asymmetric coding of envelope stimuli by ON and OFF cell subpopulations, and that downstream decoders are already tuned to such asymmetry in order to generate behavioral responses at the organismal level.

3.2. Mechanisms mediating differential effects of raphe stimulation on ON and OFF ELL pyramidal cells

Our results showing that raphe stimulation had differential effects on the responses of ON and OFF ELL pyramidal cells to envelope stimuli are surprising. This is because previous studies have found that exogenous application of serotonin had largely similar effects on the responses of ON and OFF cells, making them more excitable and thus more responsive to stimulation with EOD AMs as well as electrocommunication stimuli [41]. One possible explanation is that raphe stimulation, rather than exogenous application of serotonin, was used in the current study. However, this is unlikely to explain the difference as previous studies have found that exogenous application and raphe stimulation had qualitatively similar effects overall using stimuli other than the ones considered here [41]. Further evidence against this hypothesis is that we observed changes in the sensitivity of single ELL pyramidal cells as well as behavioral responses to envelope stimuli that were similar to those observed previously using exogenous serotonin application [43]. Thus, it is very unlikely that the differential effects of serotonin on ON and OFF ELL pyramidal cells we observed were due to raphe stimulation rather than exogenous application of serotonin.

Another possibility is that the mechanisms that mediate ELL pyramidal cell responses to envelope stimuli considered here are fundamentally different than those mediating responses to other stimuli such as EOD AMs and electrocommunication stimuli considered elsewhere. Indeed, while responses to EOD AMs and electrocommunication stimuli are due to feedforward input and can be modulated by feedback [53,54], responses to envelope stimuli at low intensities are instead mediated by feedback [55–57]. While the nature of the mechanisms by which this occurs has not yet been elucidated [58], we hypothesize that the differential effects of raphe stimulation observed here are due to ON and OFF cells differentially integrating feedback input. It is conceivable that the differential effects of serotonin on ON and OFF cells occur because OFF cells receive inhibition from local interneurons whereas ON cells receive direct excitation from electroreceptor afferents. However, results obtained showing similar effects of serotonin for ON and OFF cells both *in vitro* [40] and *in vivo* [41] suggest that the effects of serotonin on both ON and OFF cells are primarily mediated through 5-HT receptors located on the pyramidal cell membrane. Further experiments suggest that serotonin increases excitability in ON and OFF cells through inhibition of both SK and M-type potassium currents via 5-HT2 receptors [40,42]. As such, an alternative but not necessarily mutually exclusive hypothesis for the differential effects of serotonin on ON and OFF-type cells could be due to the fact that ON cells express both SK1 channels on their dendrites as well as SK2 channels on their somata, whereas OFF cells only express SK1 channels on their dendrites [59]. The presence of SK2 channels has been shown to strongly influence responses of ON cells to current injection *in vitro* in particular through burst firing [60,61], thereby suggesting that the presence of such channels can strongly influence integration of synaptic input. Moreover, serotonin application *in vitro* inhibits SK2 channels in ON ELL pyramidal cells [40] via $5HT_2$-like receptors [42]. As such, we hypothesize that the differential effects of raphe stimulation on ON and OFF ELL pyramidal cells observed in the current study are due to downregulation of SK2 channels that are present in the former but not the latter. As such, we predict that heterogeneities in envelope responses for ON cells are in part due to differential levels of expression of SK2 channels [62]. Further studies are needed to test these experimentally.

3.3. Population coding by ELL pyramidal cells: implications for behavior

While previous studies have largely focused on population coding by relying on single-unit recordings from ELL pyramidal cells (see Refs. [26,27,31,48] for review), more recent studies have started to use multi-unit recordings to investigate population coding [47]. As previously mentioned, correlations between the trial-to-trial variabilities of neural responses (i.e., noise correlations), which can only be measured using simultaneous recordings, have been found ubiquitously and can strongly influence information transmission by neural populations (see Refs. [16–18,63] for review). Noise correlations are present in the ELL and strongly depend on stimulus attributes [64]. Moreover, these can induce synergy between the activities of ELL pyramidal cells such as to enhance information transmitted about electrocommunication stimuli by ON and OFF ELL pyramidal cells [47]. In contrast, our results show that for envelope stimuli noise correlations are present but are, at best, minimally modulated by raphe stimulation and do not much influence population coding by ELL pyramidal cells. The small changes in noise correlations after raphe stimulation support the hypothesis that noise correlations in the ELL are primarily from feedforward mechanisms, such as shared input from electroreceptor afferents, as opposed to feedback [65].

While population coding by ELL pyramidal cells is generally "symmetric" in that responses of OFF cells largely mirror those of ON cells [24,66,67], our results show that this is not the case for envelope stimuli as ON cells primarily carry information. This result is surprising because previous studies have found that ON and OFF cells generally displayed similar response properties to envelopes [28, 33]. However, it is important to note that these have only considered the sensitivity to envelopes and did not quantify trial-to-trial variability. Moreover, coinciding with our findings, previous research has demonstrated that including the effects of such variability can lead to qualitatively different results than those obtained when considering sensitivity alone [68,69]. Indeed, a recent study has shown asymmetric coding of natural electrocommunication stimuli by ON and OFF cells [47]. It should furthermore be noted that our results do not imply in any way that OFF cells do not serve an important function. As mentioned above, OFF cells respond strongly to AM stimuli [54,66,70,71] and, as such, likely contribute to generating associated behavioral responses such as the jamming avoidance response [72]. Moreover, OFF cells respond strongly to a particular class of natural electrocommunication stimuli that occur during male-female interactions [53,73].

How are the activities of ELL pyramidal cells combined to give rise to behavior? Despite decades of research on this subject, how neural populations determine behavior remains poorly understood in general [19]. Our results provide new insight as to how ELL pyramidal cell responses to envelope stimuli give rise to observed behavioral responses. While changes in ELL pyramidal cell activity (e.g., by pharmacological inactivation of SK channels or via sensory adaptation) lead to changes in behavior, the relationship between neural activity and behavior is non-trivial [34,35]. This is in part due to the fact that ELL pyramidal cells tend to display high-pass tuning to envelope stimuli [28,33,35], whereas behavioral responses instead display low-pass tuning [32]. Our results showing that the activity of ON cell population best predicts behavioral responses make important predictions as to how information should be decoded. Specifically, downstream neurons should integrate input from ON cells only. There is evidence supporting such a decoding scheme. Specifically, both ON and OFF ELL pyramidal cells make excitatory synaptic connections with neurons within the midbrain torus semicircularis [74]. However, physiological studies have found that TS neurons are mostly ON-type in their responses to sensory input [75,76], which suggests that input from ON cells dominates. Finally, it should be noted that we convolved the spiking activities of different ELL pyramidal cells with separate filters that were chosen to minimize the mean square error in order to reconstruct the stimulus and behavior. As such, we assumed a combinatorial code which is in theory advantageous and has been considered in other systems [77,78]. However, how such codes are implemented in the nervous system remains problematic as neural identity must be retained [79]. Further studies are needed to investigate how the activities of ELL pyramidal cells in response to envelope stimuli are decoded by downstream brain areas to generate behavior. In particular, these should take into account the fact that there are serotonergic projections to multiple brain areas downstream of ELL including TS as well as the nucleus electrosensorius [39] that most likely play a role towards shaping behavioral responses.

3.4. Implications for other sensory systems

The electrosensory system shares many similarities with other systems including visual, auditory, and vestibular [48,80,81]. There is moreover evidence that the serotonergic system is ancient and is largely conserved across vertebrates, suggesting a common function [49]. Indeed, previous studies have shown similar effects of serotonin in neurons within the dorsal cochlear nucleus [82], which like the ELL is a cerebellar-like structure. Importantly, the time varying envelope stimuli considered here are behaviorally relevant stimuli found in other sensory modalities (visual: [83], auditory: [84,85], vestibular: [86], mechanosensory: [87]). Finally, the ON- and OFF-type cell distinction is a prominent feature in other sensory modalities (visual: [88], auditory: [89,90], olfactory: [91]) and asymmetries in their responses to sensory input have been previously observed [92–94]. Thus, while to our knowledge, this constitutes the first study to investigate the effects of serotonin on sensory coding by neural populations, it is likely that our results will be applicable to other systems.

4. Limitations of the Study

While there are many similarities between the electrosensory system of weakly electric fish and mammalian ones, there is no guarantee that our results will be directly applicable elsewhere. Further, future studies should investigate the release of serotonin occurring during more natural conditions than the artificial raphe stimulation employed here. Moreover, further studies are needed in order to understand the mechanisms by which serotonergic feedback decreases response heterogeneities in ON cells on the one hand

but increases response heterogeneities in OFF cells on the other hand.

Author contributions

M.M.M. and M.J.C. conceived and designed the experiments, M.M.M. performed the experiments, M.M.M. analyzed and interpreted the data, M.J.C. contributed reagents, materials, analysis tools or data, M.M.M. and M.J.C. wrote the paper.

Data availability statement

Data associated with this study has been deposited at All datasets and analysis files have been deposited in borealis (https://borealisdata.ca/dataset.xhtml?persistentId=doi:10.5683/SP3/VRPTUG) https://borealisdata.ca/privateurl.xhtml?token=efe713e6-a300-4889-bea0-1be409f1ca5a

Declaration of competing interest

The authors declare that they have no known competing financial interests or personal relationships that could have appeared to influence the work reported in this paper.

Acknowledgements

This research was supported by the Canadian Institutes of Health Research (MJC).

Appendix A. Supplementary data

Supplementary data to this article can be found online at https://doi.org/10.1016/j.heliyon.2023.e18315.

STAR Methods.

Key resources table

REAGENT or RESOURCE	SOURCE	IDENTIFIER
Chemicals, peptides, and recombinant proteins		
tubocurarine	Sigma-Aldrich	93750
Serotonin hydrochloride	Sigma-Aldrich	H9523
Deposited data		
Datasets and analysis files	this paper	https://borealisdata.ca/privateurl.xhtml?token=efe713e6-a300-4889-bea0-1be409f1ca5a
Experimental models: Organisms/strains		
Apteronotus leptorhynchus	local suppliers	N/A
Software		
Spike2	Cambridge Electronic Designs	https://ced.co.uk
SpikeGLX	Janelia Research Campus	http://billkarsh.github.io/SpikeGLX
Phy2	CortexLab	https://github.com/cortex-lab/phy
MATLAB	Mathworks	https://www.mathworks.com

Resource availability

Lead contact

Further information and requests for resources should be directed to the lead contact, Maurice J. Chacron (maurice.chacron@mcgill.ca).

Materials availability

This study did not generate new unique reagents.

Data and code availability

All datasets and analysis files have been deposited in borealis (https://borealisdata.ca/privateurl.xhtml?token=efe713e6-a300-4889-bea0-1be409f1ca5a).

Experimental model and subjective details

All animal procedures were approved by McGill University's animal care committee and were performed in accordance with the guidelines of the Canadian Council on Animal Care.

Animals

The South American wave-type weakly electric fish *Apteronotus leptorhynchus* was used in this study (N = 3). Animals of either sex were obtained from tropical fish suppliers and housed in groups of no more than 10 at controlled conditions (water temperature: 26–29 °C, water conductivity: 100–300 μS*cm^{-1}) according to established guidelines [95].

Surgery

Animals were immobilized for electrophysiology experiments by an intramuscular injection of tubocurarine chloride hydrate (0.1–0.5 mg, Sigma-Aldrich) and were then transferred to an experimental tank containing water from the home tank. The electric organ of *Apteronotus leptorhynchus* is neurogenic and thus, the electric organ discharge is not affected by curare. A constant flow of oxygenated water was passed through the fish's gills (10 mL*min^{-1}) via a mouth tube. The animal's head was kept slightly above the water level and locally anesthetized with lidocaine ointment (5%, AstraZeneca). Two small craniotomies were performed to access the hindbrain area for recordings in the electrosensory lateral line lobe (ELL) and the midbrain area for electrical stimulation of the raphe nuclei as done previously [41].

Recordings and electrical stimulation of serotonergic fibers

We used Neuropixels probes (Imec Inc. [14]) to record the simultaneous activity of ELL pyramidal cells as done previously [47]. The probe was inserted at an angle of 15 deg with respect to the sagittal plane and advanced 1500–2000 μm from the surface to record neurons located at depths between 400 and 1200 μm. We aimed to record neurons from the lateral segment of the ELL, as they receive the highest amount of serotonergic innervation from the dorsal raphe nuclei [39,40]. Recordings were digitalized at 30 kHz using SpikeGLX (Janelia Research Campus) and stored for offline analysis.

To investigate the effects of serotonin in a population of neurons, we simultaneously recorded neural and behavioral responses to envelopes during control conditions and after the electrical stimulation of serotonergic fibers emanating from the Raphe nuclei that innervate the ELL. We used a bipolar tungsten electrode positioned 1 mm rostral to T0, advanced 3500 μm in depth. The stimulation electrode was positioned near the target, before advancing the probe to its final position. We waited at least 30 min before starting the recording to allow the brain tissue to settle and improve recording stability. Once the experimental protocol was run for the control condition, we delivered 10 pulses (200–300 pA) at 40 Hz with each pulse lasting 0.3 ms, as done previously [41]. We tested if the electrical stimulation was successful by recording the jamming avoidance response (JAR, further described below) right before and immediately after delivering the electrical pulses, as previous studies have shown this behavioral response is increased after stimulation [41,43]. Thus, the full experimental protocol was the following: recording of control condition, JAR test, electrical stimulation of raphe, JAR test after stimulation and recording of serotonin condition.

We note that although the electrical stimulation of serotonergic fibers was localized, the perturbations it induced in the recordings made it difficult to retain the identity of all the neurons recorded from across conditions. Accordingly, for session 1 we recorded n = 13 neurons during control, n = 13 neurons after raphe stimulation and retained identity of n = 3; for session 2 we recorded n = 17 neurons during control, n = 24 after raphe stimulation and retained identity of n = 9 neurons; for session 3 we recorded n = 21 neurons during control, n = 24 after raphe stimulation and retained the identity of n = 6 neurons. Qualitatively similar results were obtained when comparing the same population of neurons and two different populations of neurons across conditions. We only show results from the analysis performed for the same population of neurons throughout this paper except in Sup Fig. 3 where ON and OFF cells were compared before and after raphe stimulation. ELL pyramidal cells were identified based on previously well-established characteristics such as firing rate and response to stimulation. For our dataset, the baseline firing rate was 16.51 ± 0.81 Hz (min: 6.23 Hz; max: 30.62 Hz), which is similar to what was found in previous studies [24,51,54,66,71,96]. We note that other cell types within the ELL such as inhibitory interneurons typically have much larger firing rates [97] and, as such, can easily be distinguished from ELL pyramidal cells.

Stimulation

Stimuli consisted of a 5–15 Hz noise (4th order Butterworth) amplitude modulation (AM) whose amplitude (i.e., envelope) was further modulated sinusoidally at 0.05 Hz, 0.1 Hz, 0.25 Hz, 0.5 Hz, 0.75 Hz and 1 Hz. We played 20 repetitions of a cycle for each envelope frequency. These envelope stimuli mimic electrical signals that arise due to relative movement between two fish [30,32] and as such, the range of envelope frequencies chosen is behaviorally relevant. Single neuron and behavioral responses to envelopes have been the subject of several recent studies (see Ref. [31] for a review). The envelope stimuli were produced by triggering a function generator to emit one cycle of a sinewave each time a cycle of the EOD was emitted, as done previously [24]. The frequency of the emitted sinewave was set slightly higher (~30 Hz) than that of the EOD, allowing for the output of the function generator to be synchronized with EOD. The emitted sinewave was subsequently multiplied by the desired AM and the resultant signal was isolated from the ground. The final signal was delivered through a pair of chloridized silver electrodes in the water located ~15 cm away from the fish perpendicular to its rostro-caudal axis. To measure the stimulus intensity, we used a small dipole placed near the fish's skin. Stimulus intensity was adjusted to produce changes in the EOD amplitude that were ~20% of the baseline level, as done in previous

studies [43,44].

We also stimulated with a low-pass filtered 0–120 Hz noise amplitude modulation to classify ELL pyramidal cells as ON- or OFF-type as described below. Thus, each control or serotonin condition consisted of recordings of a 100 s baseline period, followed by a noisy AM and lastly the envelope stimuli.

Behavior

Behavioral responses to sinusoidal envelopes consist of changes in the time-dependent EOD frequency of the fish. As mentioned above, a signal is triggered every time the fish emits a cycle of the EOD. This triggered signal or 'zero-crossings' of the EOD are converted into a binary sequence and low-pass filtered (second-order Butterworth with 0.05 Hz cutoff) to finally obtain the time-dependent EOD, as done previously [34].

The jamming avoidance response was elicited by a 4 Hz sinusoidal AM stimulus played for at least 50 s. The stimulus was presented five times with a rest period of at least 20 s between each presentation. The JAR magnitude was defined as the maximum EOD frequency elicited during stimulation relative to the EOD frequency baseline value, as done previously [41,43].

Data analysis

Spike times for each individual neuron were sorted using Kilosort [98] and manually curated using phy 2 (https://github.com/cortex-lab/phy). The spike time sequences were then converted to a binary sampled at 2 kHz, i.e., the content of a binwidth of 0.5 ms is 1 if a spike occurred and 0 otherwise. All data analysis was performed using custom codes written in Matlab (MathWorks).

ELL pyramidal cells were classified as ON or OFF according to their responses to a low-pass filtered 0–120 Hz noise amplitude modulation as done previously [47,99]. Briefly, we computed the spike triggered average (STA) by averaging stimulus segments during 1 s windows centered at the action potential times of a given neuron. We then computed the STA slope during an 8 ms window centered 8 ms before the action potential occurred to account for spike transmission delay. Neurons for which the slope was positive weare classified as ON cells, whereas those for which the slope was negative were classified as OFF cells.

We computed baseline firing rates and burst fractions from a 100 s of baseline data before presenting the stimuli. Burst fraction was defined as the ratio of the number of spikes that occurred in a burst (i.e., interspike interval $\leq$ burst threshold) to the total number of spikes. The burst threshold corresponds to the trough of the bimodal ISI distribution which was on average 10 ms. We note that this burst threshold has been used extensively in the electrosensory system [70,100–102].

To quantify neural responses to envelopes we used linear systems identification techniques to compute gain and phase as done previously [35,43,44]. Specifically, neural gain is defined as the ratio of the amplitude of the filtered firing rate response and the stimulus amplitude, measured from the dipole. The response phase is defined as the average phase at which the filtered firing rate reached its maximum relative to the peak of the stimulus waveform over each cycle divided by a period of 2π. The filtered firing rates were obtained by low-pass filtering the binary sequencies with a [10, 5, 2, 1, 0.65, 0.5] s long box car window (i.e., the filter is constant for the duration of the window and zero otherwise, see "boxcar" function in Matlab) for envelope frequencies [0.05, 0.1, 0.25, 0.5, 0.75, 1] Hz respectively. We note that these lengths correspond to one half of the envelope period for all frequencies tested.

Polar plots were generated by plotting the phase (angular coordinate) and gain (radial coordinate). From these polar plots, we computed the circular standard deviation as:

$$cir\ STD = \sqrt{-2\ log(\overline{R})}$$

where $\overline{R}$ is the mean resulting length of the trigonometric moments of the circular distribution. Note that values near 0 correspond to little variation in phase values.

To quantify the trial-to-trial variability in the firing rate response of ELL pyramidal cells to the envelope signal, we calculated the mean response from the filtered binaries across trials and subtracted this mean response from each individual trial to obtain the 'noise'. We defined the trial-to-trial variability as the mean of the absolute value of the noise across trials. The signal to noise ratio (snr) is measured as the ratio between the amplitude of the mean response and the trial-to-trial variability.

We quantified pairwise correlations between neural activities recorded simultaneously by computing the Pearson's correlation coefficient between two filtered firing rate sequences (n_i) as:

$$r_{total} = \frac{Cov(n_1 n_2)}{\sqrt{Var(n_1)Var(n_2)}}$$

To compute signal correlations, we used this equation on firing rate sequences shuffled across trials and averaged over 20 realizations of the shuffling procedure. To compute noise correlations, we used the firing rate residual sequences of the shuffling procedure. The firing rate residual sequences were obtained by subtracting the mean firing rate sequence from the firing rate for each individual trial. Since the mean firing rate sequence corresponds to the firing rate modulation due to the stimulus presentation, the residual firing rate sequence represents the component of the neural response that cannot be attributed to a given stimulus waveform (i.e., noise) as this is not constant across trials.

Stimulus reconstruction and coding fraction

An estimate of the time-varying envelope stimulus $E(t)$ was obtained from the population of ELL pyramidal cells by convolving each spike train $R_i(t)$ with a linear filter $K_i(t)$ and adding the contributions of all cells [103–106]:

$$E_{est}(t) = \sum_{i=1}^{n} \int d\tau K_i(\tau) R_i(t-\tau)$$

The filters $K_i(t)$ are chosen to minimize the mean square error ε^2 between the stimulus and its estimate:

$$\varepsilon^2 = \langle [E(t) - E_{est}(t)]^2 \rangle$$

The optimal set of filters are the solution to the following system of equations [52,107]:

$$\begin{pmatrix} P_{R1R1}(f) & P_{R1R2}(f) & \cdots & P_{R1Rn}(f) \\ P_{R2R1}(f) & P_{R2R2}(f) & \cdots & P_{R2Rn}(f) \\ \vdots & \vdots & \ddots & \vdots \\ P_{RnR1}(f) & P_{RnR2}(f) & \cdots & P_{RnRn}(f) \end{pmatrix} \begin{pmatrix} \widetilde{K}_1(f) \\ \widetilde{K}_2(f) \\ \vdots \\ \widetilde{K}_n(f) \end{pmatrix} = \begin{pmatrix} P_{ER1}(-f) \\ P_{ER2}(-f) \\ \vdots \\ P_{ERn}(-f) \end{pmatrix}$$

Where $\widetilde{K}_i(f)$ is the Fourier transform of $K_i(t)$, $P_{R_iR_j}(f)$ is the cross-spectrum between binary sequences $R_i(t)$ and $R_j(t)$ and $P_{ER_j}(-f)$ is the cross-spectrum between the stimulus $E(t)$ and binary sequence $R_i(t)$. The quality of the reconstruction was assessed by the coding fraction *cf*, defined by:

$$cf = 1 - \frac{\varepsilon}{\sigma}$$

Where σ is the standard deviation of the envelope. *cf* ranges between 0 and 1 and represents the fraction of the stimulus that is correctly estimated [52,108]. This algorithm was applied either to neural activities that were recorded from simultaneously or using the shuffled trials (see above description) in order to quantify the effects of noise correlations on coding.

Statistics

Values are reported as mean ± SE unless otherwise indicated. Statistical significance was evaluated by either a parametric Student's t-test if the data was normally distributed or non-parametric Wilcoxon signed-rank test otherwise for paired samples. When comparing unpaired samples, we used a parametric unpaired Student's t-test if the data was normally distributed or a non-parametric Wilcoxon rank sum test otherwise. Significance at the $p = 0.05$ level is indicated by "*" in all figures. Whether the data follow a normal distribution was evaluated by a Lilliefors test at the $p = 0.05$ level. Where indicated, error bars were generated by bootstrapping technique, computing 50 bootstraps taking 80% of the measured values.

References

[1] C.I. Bargmann, Beyond the connectome: how neuromodulators shape neural circuits, Bioessays 34 (2012) 458–465.
[2] E. Marder, Neuromodulation of neuronal circuits: back to the future, Neuron 76 (2012) 1–11.
[3] L.M. Hurley, D.M. Devilbiss, B.D. Waterhouse, A matter of focus: monoaminergic modulation of stimulus coding in mammalian sensory networks, Curr. Opin. Neurobiol. 14 (2004) 488–495.
[4] S.N. Jacob, H. Nienborg, Monoaminergic neuromodulation of sensory processing, Front. Neur. Circ. 12 (2018).
[5] L. Hurley, Serotonin in auditory processing, in: C.P. Müller, K.A. Cunningham (Eds.), Handbook of the Behavioral Neurobiology of Serotonin Second Edition, ELSEVIER/Academic Press, 2018.
[6] L.M. Hurley, M.R. Sullivan, From behavioral context to receptors: serotonergic modulatory pathways in the IC, Front. Neural Circ. 6 (2012) 58.
[7] B.D. Waterhouse, S.A. Azizi, R.A. Burne, D.J. Woodward, Modulation of rat cortical area 17 neuronal responses to moving visual stimuli during norepinephrine and serotonin microiontophoresis, Brain Res. 514 (1990) 276–292.
[8] G.C. Petzold, A. Hagiwara, V.N. Murthy, Serotonergic modulation of odor input to the mammalian olfactory bulb, Nat. Neurosci. 12 (2009) 784–791.
[9] L.M. Hurley, G.D. Pollak, Serotonin differentially modulates responses to tones and frequency-modulated sweeps in the inferior colliculus, J. Neurosci. 19 (1999) 8071–8082.
[10] L.M. Hurley, G.D. Pollak, Serotonin effects on frequency tuning of inferior colliculus neurons, J. Neurophysiol. 85 (2001) 828–842.
[11] L.M. Hurley, G.D. Pollak, Serotonin shifts first-spike latencies of inferior colliculus neurons, J. Neurosci. 25 (2005) 7876–7886.
[12] L.M. Hurley, G.D. Pollak, Serotonin modulates responses to species-specific vocalizations in the inferior colliculus, J. Comp. Phys. A Neuroethol. Sens. Neur. Behav. Phys. 191 (2005) 535–546.
[13] E. Lottem, D. Banerjee, P. Vertechi, D. Sarra, M.O. Lohuis, Z.F. Mainen, Activation of serotonin neurons promotes active persistence in a probabilistic foraging task, Nat. Commun. 9 (2018) 1000.
[14] J.J. Jun, N.A. Steinmetz, J.H. Siegle, D.J. Denman, M. Bauza, B. Barbarits, A.K. Lee, C.A. Anastassiou, A. Andrei, C. Aydin, et al., Fully integrated silicon probes for high-density recording of neural activity, Nature 551 (2017) 232–236.
[15] S. Panzeri, J.H. Macke, J. Gross, C. Kayser, Neural population coding: combining insights from microscopic and mass signals, Trends Cognit. Sci. 19 (2015) 162–172.
[16] A. Kohn, R. Coen-Cagli, I. Kanitscheider, A. Pouget, Correlations and neuronal population information, Annu. Rev. Neurosci. 39 (2016) 237–256.
[17] S. Panzeri, M. Moroni, H. Safaai, C.D. Harvey, The structures and functions of correlations in neural population codes, Nat. Rev. Neurosci. 23 (2022) 551–567.
[18] B.B. Averbeck, P.E. Latham, A. Pouget, Neural correlations, population coding and computation, Nat. Rev. Neurosci. 7 (2006) 358–366.
[19] A.E. Urai, B. Doiron, A.M. Leifer, A.K. Churchland, Large-scale neural recordings call for new insights to link brain and behavior, Nat. Neurosci. 25 (2022) 11–19.
[20] R.W. Turner, L. Maler, M. Burrows, Electroreception and electrocommunication, J. Exp. Biol. 202 (1999) 1167–1458.

[21] M.G. Metzen, E.S. Fortune, M.J. Chacron, Physiology of tuberous electrosensory systems, in: Reference Module in Life Sciences, Elsevier, 2017.
[22] C. Bell, L. Maler, in: T.H. Electroreception, C.D. Bullock, A.N. Hopkins, Popper, R.R. Fay (Eds.), Central Neuroanatomy of Electrosensory Systems in Fish, Springer, New York, 2005, pp. 68–111.
[23] J. Saunders, J. Bastian, The physiology and morphology of two classes of electrosensory neurons in the weakly electric fish *Apteronotus Leptorhynchus*, J. Comp. Physiol. 154 (1984) 199–209.
[24] J. Bastian, M.J. Chacron, L. Maler, Receptive field organization determines pyramidal cell stimulus-encoding capability and spatial stimulus selectivity, J. Neurosci. 22 (2002) 4577–4590.
[25] M. Haggard, M.J. Chacron, Coding of object location by heterogeneous neural populations with spatially dependent correlations in weakly electric fish, PLoS Comput. Biol. 19 (2023), e1010938.
[26] L. Maler, Receptive field organization across multiple electrosensory maps. I. Columnar organization and estimation of receptive field size, J. Comp. Neurol. 516 (2009) 376–393.
[27] R. Krahe, L. Maler, Neural maps in the electrosensory system of weakly electric fish, Curr. Opin. Neurobiol. 24 (2014) 13–21.
[28] C.G. Huang, M.J. Chacron, SK channel subtypes enable parallel optimized coding of behaviorally relevant stimulus attributes: a review, Channels 11 (2017) 281–304.
[29] M.G. Metzen, M.J. Chacron, Envelope coding and processing: implications for perception and behavior, in: B. Carlson, J. Sisneros, A. Popper, R. Fay (Eds.), Electroreception: Fundamental Insights from Comparative Approaches, Springer, Cham, 2019, pp. 251–277.
[30] S.A. Stamper, E.S. Fortune, M.J. Chacron, Perception and coding of envelopes in weakly electric fishes, J. Exp. Biol. 216 (2013) 2393–2402.
[31] M.G. Metzen, M.J. Chacron, Envelope Coding and Processing: Implications for Perception and Behavior, Springer International Publishing, 2019, pp. 251–277.
[32] M.G. Metzen, M.J. Chacron, Weakly electric fish display behavioral responses to envelopes naturally occurring during movement: implications for neural processing, J. Exp. Biol. 217 (2014) 1381–1391.
[33] C.G. Huang, M.J. Chacron, Optimized parallel coding of second-order stimulus features by heterogeneous neural populations, J. Neurosci. 36 (2016) 9859–9872.
[34] C.G. Huang, M.G. Metzen, M.J. Chacron, Descending pathways mediate adaptive optimized coding of natural stimuli in weakly electric fish, Sci. Adv. 5 (2019), eaax2211.
[35] C.G. Huang, Z.D. Zhang, M.J. Chacron, Temporal decorrelation by SK channels enables efficient neural coding and perception of natural stimuli, Nat. Commun. 7 (2016) 11353.
[36] M.G. Metzen, M.J. Chacron, Neural heterogeneities determine response characteristics to second-, but not first-order stimulus features, J. Neurosci. 35 (2015) 3124–3138.
[37] J.W. Middleton, A. Longtin, J. Benda, L. Maler, The cellular basis for parallel neural transmission of a high-frequency stimulus and its low-frequency envelope, Proc. Natl. Acad. Sci. USA 103 (2006) 14596–14601.
[38] A. Longtin, J.W. Middleton, J. Cieniak, L. Maler, Neural dynamics of envelope coding, Math. Biosci. 214 (2008) 87–99.
[39] S.A. Johnston, L. Maler, B. Tinner, The distribution of serotonin in the brain of *Apteronotus leptorhynchus*: an immunohistochemical study, J. Chem. Neuroanat. 3 (1990) 429–465.
[40] T. Deemyad, L. Maler, M.J. Chacron, Inhibition of SK and M channel-mediated currents by 5-HT enables parallel processing by bursts and isolated spikes, J. Neurophysiol. 105 (2011) 1276–1294.
[41] T. Deemyad, M.G. Metzen, Y. Pan, M.J. Chacron, Serotonin selectively enhances perception and sensory neural responses to stimuli generated by same-sex conspecifics, Proc. Natl. Acad. Sci. USA 110 (2013) 19609–19614.
[42] E.A. Larson, M.G. Metzen, M.J. Chacron, Serotonin modulates electrosensory processing and behavior via 5-HT2-like receptors, Neuroscience 271 (2014) 108–118.
[43] M.M. Marquez, M.J. Chacron, Serotonin modulates optimized coding of natural stimuli through increased neural and behavioural responses via enhanced burst firing, J. Physiol. 598 (2020) 1573–1589.
[44] M.M. Marquez, M.J. Chacron, Serotonergic modulation of sensory neuron activity and behavior in Apteronotus albifrons, Front. Integr. Neurosci. 14 (2020) 38.
[45] M.M. Marquez, M.J. Chacron, Serotonin and sensory processing, in: C. Muller, K. Cunningham (Eds.), Handbook of the Behavioral Neurobiology of Serotonin vol. 31, Academic Press, 2020, pp. 449–459.
[46] M.G. Metzen, M.J. Chacron, Population coding of natural electrosensory stimuli by midbrain neurons, J. Neurosci. 41 (2021) 3822–3841.
[47] Z. Wang, M.J. Chacron, Synergistic population coding of natural communication stimuli by hindbrain electrosensory neurons, Sci. Rep. 11 (2021) 10840.
[48] S.E. Clarke, A. Longtin, L. Maler, Contrast coding in the electrosensory system: parallels with visual computation, Nat. Rev. Neurosci. 16 (2015) 733–744.
[49] A. Parent, Comparative anatomy of the serotoninergic systems, J. de physiologie 77 (2–3) (1981) 147–156.
[50] V. Hofmann, M.J. Chacron, Neural On- and Off-type heterogeneities improve population coding of envelope signals in the presence of stimulus-induced noise, Sci. Rep. 10 (2020) 10194.
[51] M.M. Marquez, M.J. Chacron, Serotonin modulates optimized coding of natural stimuli through increased neural and behavioural responses via enhanced burst firing, J. Physiol. 598 (2020) 1573–1589.
[52] F. Rieke, D. Warland, R.R. de Ruyter van Steveninck, W. Bialek, Spikes: Exploring the Neural Code, MIT, Cambridge, MA, 1996.
[53] G. Marsat, A. Longtin, L. Maler, Cellular and circuit properties supporting different sensory coding strategies in electric fish and other systems, Curr. Opin. Neurobiol. 22 (2012) 686–692.
[54] M.J. Chacron, L. Maler, J. Bastian, Feedback and feedforward control of frequency tuning to naturalistic stimuli, J. Neurosci. 25 (2005) 5521–5532.
[55] M.G. Metzen, C.G. Huang, M.J. Chacron, Descending pathways generate perception of and neural responses to weak sensory input, PLoS Biol. 16 (2018), e2005239.
[56] C.G. Huang, M.G. Metzen, M.J. Chacron, Feedback optimizes neural coding and perception of natural stimuli, Elife 7 (2018), e38935.
[57] V. Hofmann, M.J. Chacron, Novel functions of feedback in electrosensory processing, Front. Integr. Neurosci. 13 (2019) 52.
[58] C. Kim, M.J. Chacron, Lower baseline variability gives rise to lower detection thresholds in midbrain than hindbrain electrosensory neurons, Neuroscience 448 (2020) 43–54.
[59] L.D. Ellis, L. Maler, R.J. Dunn, Differential distribution of SK channel subtypes in the brain of the weakly electric fish Apteronotus leptorhynchus, J. Comp. Neurol. 507 (2008) 1964–1978.
[60] L.D. Ellis, W.H. Mehaffey, E. Harvey-Girard, R.W. Turner, L. Maler, R.J. Dunn, SK channels provide a novel mechanism for the control of frequency tuning in electrosensory neurons, J. Neurosci. 27 (2007) 9491–9502.
[61] W.H. Mehaffey, L. Maler, R.W. Turner, Intrinsic frequency tuning in ELL pyramidal cells varies across electrosensory maps, J. Neurophysiol. 99 (2008) 2641–2655.
[62] L.D. Ellis, L. Maler, R.J. Dunn, Differential distribution of SK channel subtypes in the brain of the weakly electric fish Apteronotus leptorhynchus, J. Comp. Neurol. 507 (2008) 1964–1978.
[63] V. Hofmann, M.J. Chacron, Population coding and correlated variability in electrosensory pathways, Front. Integr. Neurosci. 12 (2018) 56.
[64] M.J. Chacron, J. Bastian, Population coding by electrosensory neurons, J. Neurophysiol. 99 (2008) 1825–1835.
[65] V. Hofmann, M.J. Chacron, Differential receptive field organizations give rise to nearly identical neural correlations across three parallel sensory maps in weakly electric fish, PLoS Comput. Biol. 13 (2017), e1005716.
[66] R. Krahe, J. Bastian, M.J. Chacron, Temporal processing across multiple topographic maps in the electrosensory system, J. Neurophysiol. 100 (2008) 852–867.
[67] M.G. Metzen, V. Hofmann, M.J. Chacron, Neural correlations enable invariant coding and perception of natural stimuli in weakly electric fish, Elife 5 (2016), e12993.
[68] M.J. Chacron, L. Maler, J. Bastian, Electroreceptor neuron dynamics shape information transmission, Nat. Neurosci. 8 (2005) 673–678.

[69] S.G. Sadeghi, M.J. Chacron, M.C. Taylor, K.E. Cullen, Neural variability, detection thresholds, and information transmission in the vestibular system, J. Neurosci. 27 (2007) 771–781.
[70] O. Avila-Akerberg, R. Krahe, M.J. Chacron, Neural heterogeneities and stimulus properties affect burst coding in vivo, Neuroscience 168 (2010) 300–313.
[71] M.J. Chacron, Nonlinear information processing in a model sensory system, J. Neurophysiol. 95 (2006) 2933–2946.
[72] W. Heiligenberg, Neural Nets in Electric Fish, MIT Press, Cambridge MA, 1991.
[73] G. Marsat, L. Maler, Neural heterogeneity and efficient population codes for communication signals, J. Neurophysiol. 104 (2010) 2543–2555.
[74] C.E. Carr, L. Maler, A Golgi study of the cell types of the dorsal torus semicircularis of the electric fish Eigenmannia: functional and morphological diversity in the midbrain, J. Comp. Neurol. 235 (1985) 207–240.
[75] K. Vonderschen, M.J. Chacron, Sparse and dense coding of natural stimuli by distinct midbrain neuron subpopulations in weakly electric fish, J. Neurophysiol. 106 (2011) 3102–3118.
[76] P. McGillivray, K. Vonderschen, E.S. Fortune, M.J. Chacron, Parallel coding of first- and second-order stimulus attributes by midbrain electrosensory neurons, J. Neurosci. 32 (2012) 5510–5524.
[77] S.S. Hohl, K.S. Chaisanguanthum, S.G. Lisberger, Sensory population decoding for visually guided movements, Neuron 79 (2013) 167–179.
[78] J.D. Seelig, V. Jayaraman, Neural dynamics for landmark orientation and angular path integration, Nature 521 (2015) 186–191.
[79] T.O. Sharpee, J.A. Berkowitz, Linking neural responses to behavior with information-preserving population vectors, Curr. Opin. Behav. Sci. 29 (2019) 37–44.
[80] D.E. Mitchell, A. Kwan, J. Carriot, M.J. Chacron, K.E. Cullen, Neuronal variability and tuning are balanced to optimize naturalistic self-motion coding in primate vestibular pathways, Elife 7 (2018), e43019.
[81] I. Mackrous, J. Carriot, K.E. Cullen, M.J. Chacron, Neural variability determines coding strategies for natural self-motion in macaque monkeys, Elife 9 (2020), e57484.
[82] R.A. Felix 2nd, C.J. Elde, A.A. Nevue, C.V. Portfors, Serotonin modulates response properties of neurons in the dorsal cochlear nucleus of the mouse, Hear. Res. 344 (2017) 13–23.
[83] I. Mareschal, C.L. Baker Jr., Cortical processing of second-order motion, Vis. Neurosci. 16 (1999) 527–540.
[84] R.V. Shannon, F.G. Zeng, J. Wygonski, Speech recognition with altered spectral distribution of envelope cues, J. Acoust. Soc. Am. 104 (1998) 2467–2476.
[85] P. Heil, Coding of temporal onset envelope in the auditory system, Speech Commun. 41 (2003) 123–134.
[86] J. Carriot, M. Jamali, K.E. Cullen, M.J. Chacron, Envelope statistics of self-motion signals experienced by human subjects during everyday activities: implications for vestibular processing, PLoS One 12 (2017), e0178664.
[87] A.E.B. Chang, A.G. Vaughan, R.I. Wilson, A mechanosensory circuit that mixes opponent channels to produce selectivity for complex stimulus features, Neuron 92 (2016) 888–901.
[88] H. Wassle, Parallel processing in the mammalian retina, Nat. Rev. Neurosci. 5 (2004) 747–757.
[89] N. Suga, Single unit activity in cochlear nucleus and inferior colliculus of echo-locating bats, J. Physiol. 172 (1964) 449–474.
[90] J. He, On and off pathways segregated at the auditory thalamus of the Guinea pig, J. Neurosci. 21 (2001) 8672–8679.
[91] S.H. Chalasani, N. Chronis, M. Tsunozaki, J.M. Gray, D. Ramot, M.B. Goodman, C.I. Bargmann, Dissecting a circuit for olfactory behaviour in Caenorhabditis elegans, Nature 450 (2007) 63–70.
[92] Y. Jiang, G. Purushothaman, V.A. Casagrande, The functional asymmetry of ON and OFF channels in the perception of contrast, J. Neurophysiol. 114 (2015) 2816–2829.
[93] A. Leonhardt, G. Ammer, M. Meier, E. Serbe, A. Bahl, A. Borst, Asymmetry of Drosophila ON and OFF motion detectors enhances real-world velocity estimation, Nat. Neurosci. 19 (2016) 706–715.
[94] M.A. Freed, Asymmetry between ON and OFF alpha ganglion cells of mouse retina: integration of signal and noise from synaptic inputs, J. Physiol. 595 (2017) 6979–6991.
[95] E.M. Hitschfeld, S.A. Stamper, K. Vonderschen, E.S. Fortune, M.J. Chacron, Effects of restraint and immobilization on electrosensory behaviors of weakly electric fish. ILAR journal/National Research Council, Inst. Labor. Ani. Res. 50 (2009) 361–372.
[96] J. Bastian, M.J. Chacron, L. Maler, Plastic and non-plastic cells perform unique roles in a network capable of adaptive redundancy reduction, Neuron 41 (2004) 767–779.
[97] J. Bastian, J. Courtwright, J. Crawford, Commissural neurons of the electrosensory lateral line lobe of *Apteronotus Leptorhynchus*. Morphological and physiological characteristics, J. Comp. Physiol. 173 (1993) 257–274.
[98] N.A. Steinmetz, C. Aydin, A. Lebedeva, M. Okun, M. Pachitariu, M. Bauza, M. Beau, J. Bhagat, C. Böhm, M. Broux, et al., Neuropixels 2.0: a miniaturized high-density probe for stable, long-term brain recordings, Science 372 (2021).
[99] V. Hofmann, M.J. Chacron, Neuronal On- and Off-type heterogeneities improve population coding of envelope signals in the presence of stimulus-induced noise, Sci. Rep. 10 (2020) 10194.
[100] A.M.M. Oswald, M.J. Chacron, B. Doiron, J. Bastian, L. Maler, Parallel processing of sensory input by bursts and isolated spikes, J. Neurosci. 24 (2004) 4351–4362.
[101] M.M. Marquez, M.J. Chacron, Serotonin selectively increases detectability of motion stimuli in the electrosensory system, eNeuro 5 (2018) e0013–e0018, 2018.
[102] N. Khosravi-Hashemi, E.S. Fortune, M.J. Chacron, Coding movement direction by burst firing in electrosensory neurons, J. Neurophysiol. 106 (2011) 1954–1968.
[103] D.K. Warland, P. Reinagel, M. Meister, Decoding visual information from a population of retinal ganglion cells, J. Neurophysiol. 78 (1997) 2336–2350.
[104] Y. Dan, J.-M. Alonso, W.M. Usrey, R.C. Reid, Coding of visual information by precisely correlated spikes in the lateral geniculate nucleus, Nat. Neurosci. 1 (1998) 501–507.
[105] R. Krahe, G. Kreiman, F. Gabbiani, C. Koch, W. Metzner, Stimulus encoding and feature extraction by multiple sensory neurons, J. Neurosci. 22 (2002) 2374–2382.
[106] C. Massot, M.J. Chacron, K.E. Cullen, Information transmission and detection thresholds in the vestibular nuclei: single neurons versus population encoding, J. Neurophysiol. 105 (2011) 1798–1814.
[107] P. Dayan, L.F. Abbott, Theoretical Neuroscience: Computational and Mathematical Modeling of Neural Systems, MIT press, Cambridge, MA, 2001.
[108] F. Gabbiani, W. Metzner, R. Wessel, C. Koch, From stimulus encoding to feature extraction in weakly electric fish, Nature 384 (1996) 564–567.